International Journal of Greenhouse Gas Control 4 (2010) 668–678

Contents lists available at ScienceDirect

International Journal of Greenhouse Gas Control

journal homepage: www.elsevier.com/locate/ijggc

Dual poroelastic response of a coal seam to CO_2 injection

Yu Wu[a,b], Jishan Liu[b,*], Derek Elsworth[c], Zhongwei Chen[b], Luke Connell[d], Zhejun Pan[d]

[a] State Key Laboratory for Geomechanics and Deep Underground Engineering, China University of Mining and Technology, Xuzhou, Jiangsu, 221008, China
[b] School of Mechanical Engineering, The University of Western Australia, WA 6009, Australia
[c] Department of Energy and Mineral Engineering, Penn State University, USA
[d] CSIRO Petroleum Resources, Private Bag 10, Clayton South, Victoria 3169, Australia

ARTICLE INFO

Article history:
Received 3 April 2009
Received in revised form 25 January 2010
Accepted 23 February 2010
Available online 20 March 2010

Keywords:
CO_2 sequestration
Dual poroelasticity
Numerical modelling
Gas sorption
Coal swelling

ABSTRACT

Although the influence of gas sorption-induced coal deformation on porosity and permeability has been widely recognized, prior studies are all under conditions of no change in overburden stress and effective stress-absent where effective stresses scale inversely with applied pore pressures. Here we extend formalism to couple the transport and sorption of a compressible fluid within a dual-porosity medium where the effects of deformation are rigorously accommodated. This relaxes the prior assumption that total stresses remain constant and allows exploration of the full range of mechanical boundary conditions from invariant stress to restrained displacement. Evolution laws for permeability and related porosity are defined at the micro-scale and applied to both matrix and an assumed orthogonal, regular and continuous fracture system. Permeability and porosity respond to changes in effective stress where sorption-induced strains may build total stresses and elevate effective stresses. Gas accumulation occurs in both free- and adsorbed-phases and due to effective grain and skeletal compressibilities. A finite element model is applied to quantify the net change in permeability, the gas flow, and the resultant deformation in a prototypical coal seam under in situ stresses. Results illustrate how the CO_2 injectivity is controlled both by the competition between the effective stress and the gas transport induced volume change within the matrix system and by the dynamic interaction between the matrix system and the fracture system. For typical parameters, initial injection-related increases in permeability due to reduced effective stresses may endure for days to years but are ultimately countered by long-term reductions in permeability which may decline by an order of magnitude. Models suggest the crucial role of stresses and the dynamic interaction between matrix and fractures in correctly conditioning the observed response.

1. Introduction

With the growing international concern over the issue of global warming, geological sequestration of CO_2 is a significant contender in the mix of a greenhouse mitigation options. CO_2 sequestration in deep coal seams has attracted attention as a method of reducing the output of greenhouse gases to the atmosphere (Gale and Freund, 2001). The coal serves as a receptor for the injected CO_2 which is sequestered in the naturally fractured medium. The micro-pores and pores in the coal matrix provide the main storage space for gas and the micro-fractures through macro-fractures comprise rapid pathways for gas seepage and migration. In addition, sorption-induced strain of the coal matrix can change the porosity, the permeability and the storage capacity of coal seam via feedbacks to in situ stresses and displacement constraints. Correspondingly, the evolution of in situ stress conditions have an important influence on reservoir response and capacity for CO_2 storage, inferring that both flow and mechanical interactions should be followed in realistic simulations of behavior. This study addresses this complex dynamic problem associated with the deep sequestration of CO_2 in coal seams, incorporating realistic models of gas flow and coal deformation as a dual-porosity medium.

For dual-porosity media the porous or micro-porous matrix is the principal reservoir for the interstitial fluid either as a liquid or a gas and the interconnected fracture network provides access to these matrix blocks. Dual-porosity representations (Barenblatt et al., 1960; Warren and Root, 1963) include the response of these two principal components only—release from storage in the porous matrix and transport in the fractured network. Conversely, dual permeability or multiple permeability models represent the porosity and permeability of all constituent components (Bai et al., 1993) including the role of sorption (Bai et al., 1997) and of multiple fluids (Douglas et al., 1991). Traditional flow models accommodate the transport response as overlapping continua but neglect mechanical effects. In situations where mechanical effects are important, this behavior can be included in the response. Conceptualizations

* Corresponding author. Tel.: +61 8 6488 7205.
E-mail address: Jishan@cyllene.uwa.edu.au (J. Liu).

1750-5836/$ – see front matter © 2010 Elsevier Ltd. All rights reserved.
doi:10.1016/j.ijggc.2010.02.004

include analytical models for dual-porosity media with averaged elastic components (Aifantis, 1977), their numerical implementation, and models including the component constitutive response for dual (Elsworth and Bai, 1992; Bai and Elsworth, 2000) and multi-porous (Bai et al., 1993) media. Such models have been applied to represent the response of permeability evolution (Ouyang and Elsworth, 1993; Liu and Elsworth, 1999) in deforming aquifers (Bai and Elsworth, 1994; Liu and Elsworth, 1998) and reservoirs (Bai et al., 1995), to accommodate gas flow (Zhao et al., 2004) and to evaluate the response to external forcing by human-induced effects (Liu and Elsworth, 1999) and by earth tide (Pili et al., 2004) and other mechanical influences.

All of these previous models were developed primarily for the flow of slightly compressible liquids without sorption, and are not applicable to the flow of compressible fluids such as CO_2 and where gas sorption is the dominant mechanism of storage. Gas sorption and dissolution may cause the coal matrix to swell and/or shrink and may significantly change the specific surface areas and total macro-pore volume of the coal matrix. An increase in gas pressure results in sorption to the coal matrix and a concomitant decrease in effective stress and increase in permeability (under constant total stresses). This increase in permeability may be countered by adsorption-induced swelling of the coal matrix if displacement is restrained (Cui et al., 2004), necessitating that the correct stress path is followed if meaningful predictions of permeability evolution are to be obtained.

The net change in permeability accompanying gas sequestration is controlled competitively by the influence of effective stresses and matrix swelling, again controlled by the boundary conditions applied locally between the end-members of null changes in either mean stress or volume strain (Zhang et al., 2008). When CO_2 injection begins, the gas flows into the cleats first, and then diffuses into the matrix due to the gradient. The gas flowing through the cleats is considered to be gas seepage controlled by the permeability of fracture in the coal seam (Harpalani and Chen, 1997). But the gas diffusing in the matrix is controlled by both the permeability and the adsorption. Most of the gas is stored within micro-pores in the absorbed state in matrix. Experimental results have shown that gas sorption generally follows a Langmuir isotherm (Clarkson and Bustin, 1999a,b; Faiz et al., 2007). The overall influences of the adsorbed gas and effective stress on coal permeability were investigated through experimental (Harpalani and Schraufnagel, 1990; Harpalani and Chen, 1997; Seidle and Huitt, 1995), theoretical (Gray, 1987; Sawyer, 1990; Seidle and Huitt, 1995; Palmer and Mansoori, 1998; Pekot and Reeves, 2003; Shi and Durucan, 2003, 2005) and field (Clarkson and Bustin, 1999a,b) observations. Although, these studies have improved our understanding of the possible causes of permeability changes, they do not include the unique characteristic of coal as a typical dual-porosity system with important coupling between mechanical and transport behaviors. Therefore, these studies cannot represent the true dynamics between coal deformation, gas transport in the matrix system, and gas transport in the fracture system.

CO_2 injection into a coal seam induces complex mechanical, physical and chemical interactions. Although the influence of gas sorption-induced coal deformation on porosity and permeability has been widely studied, these studies are all under the conditions of no change in overburden stress and effective stress-absent. According to the principle of effective stress, the induced coal deformation is determined by the change in effective stress, which can be replaced by the change in pore pressure, under the assumption of null change in total stress. This is why terms representing effective stress or total stress are absent in all of these existing permeability models. In our previous work (Zhang et al., 2008), this assumption was relaxed and a new porosity and permeability model was derived. This model was also applied to quantify the net change in permeability, the gas flow, and the resultant deformation in a coal seam. In this work, a single porosity and permeability model was modified to represent both the primary medium (coal matrix) and the secondary medium (fractures), and implemented into a fully coupled model incorporating coal deformation, CO_2 flow and transport in the matrix system, and CO_2 flow and transport in the fracture system. The novel dual poroelastic model was applied to quantify the mechanical responses of coal seams to CO_2 injection under in situ stress conditions.

2. Governing equations

In the following, a set of field equations for coal deformation and gas flow are defined. These field equations are coupled through new porosity and permeability models for coal matrix and fractures. These derivations are based on the following assumptions:

(1) Coal is a dual poroelastic continuum.
(2) Strains are infinitesimal.
(3) Gas contained within the pores is ideal, and its viscosity is constant under isothermal conditions.
(4) Conditions are isothermal.
(5) Coal is saturated by gas.
(6) Compositions of the gas are not competitive, i.e., only one gas component is considered at a time.

In the following derivations, the coal is conceptualized as in Fig. 1. It consists of coal matrix and fractures. The cubic matrix length and the fracture aperture are represented by a and b, respectively. K_n is the fracture stiffness, and σ_e is the effective stress.

2.1. Coal seam deformation

For all equations, traditional conventions are used: a comma followed by subscripts denotes differentiation with respect to spatial coordinates and repeated indices in the same expression imply summation over the range of the indices.

The strain–displacement relationship is defined as:

$$\varepsilon_i = \frac{1}{2}(u_{i,j} + u_{j,i}) \tag{1}$$

where ε_i is the component of the total strain tensor and u_i is the component of displacement. The equilibrium equation with self weight and neglecting inertial effects is given as

$$\sigma_i + f_{,i} = 0 \tag{2}$$

where σ_i is the component of the total stress tensor and $f_{,i}$ is the component of body force.

The gas sorption-induced strain, ε_s, is assumed to result in volumetric strain only. Its effects on all three normal components of strain are the same. On the basis of poroelasticity and by making

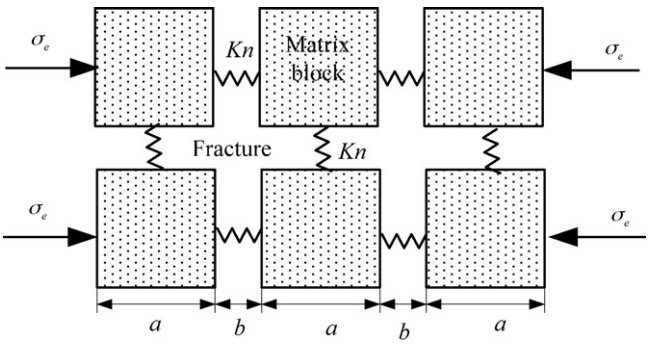

Fig. 1. Dual-porosity fractured medium.

an analogy between thermal contraction and matrix shrinkage, the constitutive relation for the deformed coal seam becomes

$$\varepsilon_i = \frac{1}{2G}\sigma_i - \left(\frac{1}{6G} - \frac{1}{9K}\right)\sigma_k\delta_{ij} + \frac{\alpha}{3K}p_m\delta_{ij} + \frac{\beta}{3K}p_f\delta_{ij} + \frac{\varepsilon_s}{3}\delta_{ij} \quad (3)$$

For the dual-porosity model, the mechanical properties of coal are affected by the fracture. The elastic parameters for Eq. (3) can be written as

$$C_1 = \frac{1}{E}, \qquad C_2 = \frac{1}{Kn \cdot a} \quad (4)$$

$$D = \frac{1}{C_1 + C_2} \quad (5)$$

$$G = \frac{D}{2(1+\nu)} \quad (6)$$

$$K = \frac{D}{2(1-2\nu)} \quad (7)$$

$$\alpha = 1 - \frac{K}{Ks} \quad (8)$$

$$\beta = 1 - \frac{K}{Kn \cdot a} \quad (9)$$

where E is elastic modulus, G is shear stiffness, σ_k are the components of the mean stress, p is gas pressure, the subscript m represents the matrix and f the fracture system, ε_s is the sorption strain, α, β are the Biot coefficients (Biot, 1941), K is the bulk modulus, Ks is the grain elastic modulus, Kn is the normal stiffness of individual fractures and δ_{ij} is the Kronecker delta.

Combining Eqs. (1)–(3) yields the Navier-type equation:

$$Gu_{i,kk} + \frac{G}{1-2\nu}u_{k,ki} - \alpha p_{m,i} - \beta p_{f,i} - K\varepsilon_{s,i} + f_{,i} = 0 \quad (10)$$

This equation is the governing equation for coal deformation. In these equations, three variables, p_m (gas pressure in the matrix), p_f (gas pressure in the fracture), and ε_s (gas sorption strain), are linked to gas flow equations as derived in the following section.

2.2. Gas flow

The mass balance equation for the gas phase is defined as

$$\frac{\partial m}{\partial t} + \nabla \cdot (\rho_g \vec{q}_g) = Q_s \quad (11)$$

Here, m is the gas content including free-phase gas and adsorbed gas, ρ_g is the gas density, $\vec{q}_g$ is the Darcy's velocity vector, Q_s is the gas source, and t is the time. It is assumed that gas sorption take places in the matrix system only. Therefore, the gas contents in the matrix and the fracture are defined as

$$m_m = \rho_{gm}\phi_m + \rho_{ga}\rho_c\frac{V_L p_m}{p_m + p_L} \quad (12)$$

$$m_f = \rho_{gf}\phi_f \quad (13)$$

Respectively, the subscripts represent m for matrix, f for fracture, g for gas, and c for coal. ϕ is porosity, ρ_{ga} is the gas density at standard conditions, V_L represents the Langmuir volume constant, p_L represents the Langmuir pressure. According to the ideal gas law, the gas density can be defined as,

$$\rho_g = \frac{M_g}{RT}p \quad (14)$$

Here, M_g is the molecular mass of the gas, R is the universal gas constant, and T is the absolute gas temperature.

Assuming the effect of gravity is relatively small and can be neglected, the Darcy volumetric flow rate can be defined as follows,

$$\vec{q}_g = -\frac{k}{\mu}\nabla \cdot p \quad (15)$$

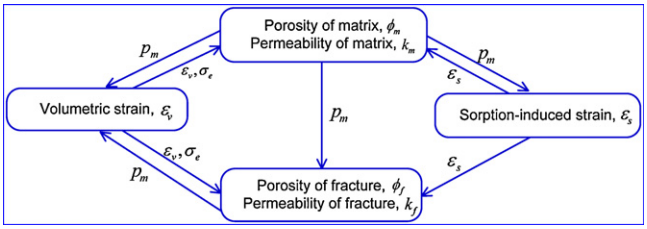

Fig. 2. Schematic of inter-relations between pressure in the matrix, p_m, pressure in the fracture, p_f, mechanical volumetric strain, ε_v, effective stress, σ_e, sorption-induced volumetric strain, ε_s, matrix and fracture porosities, ϕ_m and ϕ_f, and matrix and fracture permeability, k_m and k_f.

where k is the permeability of the coal and μ is the viscosity of the gas. Substituting Eqs. (12)–(15) into Eq. (11), the governing equations for gas flow in a dual-porosity medium are obtained as

$$\left[\phi_m + p_a\rho_c\frac{V_L p_L}{(p_m + p_L)^2}\right]\frac{\partial p_m}{\partial t} + p_m\frac{\partial \phi_m}{\partial t} + \nabla \cdot \left(-\frac{k_m}{\mu}p_m\nabla \cdot p_m\right) = \omega(p_f - p_m) \quad (16)$$

$$\phi_f\frac{\partial p_f}{\partial t} + p_f\frac{\partial \phi_f}{\partial t} + \nabla \cdot \left(-\frac{k_f}{\mu}p_f\nabla \cdot p_f\right) = -\omega(p_f - p_m) \quad (17)$$

where p_a is standard atmospheric pressure, and ω is the transfer coefficient between matrix and fracture, defined as

$$\omega = 8\left(1 + \frac{2}{a^2}\right)\frac{k_m}{\mu}. \quad (18)$$

In Eqs. (16) and (17), the porosities for matrix and fracture, ϕ_m and ϕ_f, and the permeability for the matrix and the fracture, k_m and k_f change with the mean effective stress, σ_e, and the sorption-induced strain, ε_s. In the coal deformation equation (Eq. (10)), p_m (gas pressure in the matrix), p_f (gas pressure in the fracture), and ε_s (gas sorption strain), are linked to the gas flow equations. The inter-relations between these parameters are summarized in Fig. 2 including the following cross-couplings to accommodate:

(1) Dynamic porosity evolution in the matrix
(2) Dynamic porosity evolution in the fractures
(3) Dynamic permeability evolution in the matrix
(4) Dynamic permeability evolution in the fractures

and are presented in the following sections.

2.3. Cross-couplings

2.3.1. Dynamic porosity model for matrix

The porosity model for the matrix is defined as (Zhang et al., 2008),

$$\phi_m = \frac{1}{1+S}[(1+S_0)\phi_{m0} + \alpha(S - S_0)] \quad (19)$$

where

$$S = \varepsilon_v + \frac{p_m}{Ks} - \varepsilon_s \quad (20)$$

$$S_0 = \frac{p_{m0}}{Ks} - \varepsilon_L\frac{p_{m0}}{p_{m0} + p_L} \quad (21)$$

where ε_v is the volumetric strain defined as,

$$\varepsilon_v = \frac{\sigma_e^m}{K} + \varepsilon_s \quad (22)$$

where ε_s is the sorption-induced strain. The sorption-induced volumetric strain ε_s is fitted onto Langmuir-type curves and has been

verified through experiments (Harpalani and Schraufnagel, 1990; Robertson and Christiansen, 2005). The Langmuir-type equation is defined as

$$\varepsilon_s = \varepsilon_L \frac{p_m}{p_m + p_L} \tag{23}$$

where the Langmuir volumetric strain, ε_L, is a constant representing the volumetric strain at infinite pore pressure and the Langmuir pressure constant, p_L, represents the pore pressure at which the measured volumetric strain is equal to $0.5\varepsilon_L$.

2.3.2. Dynamic permeability model for matrix

Experiments also show that the permeability of coal matrix varies with porosity as (Liu et al., 1999; Cui and Bustin, 2005):

$$\frac{k}{k_0} = \left(\frac{\phi}{\phi_0}\right)^3. \tag{24}$$

Substituting Eq. (14) into Eq. (24) gives

$$\frac{k_m}{k_{m0}} = \left(\frac{1}{\phi_0(1+S)}[(1+S_0)\phi_0 + \alpha(S-S_0)]\right)^3. \tag{25}$$

Here, the subscript 0 denotes the initial value of the variable and subscript m denotes matrix. As shown in Eq. (25), the matrix permeability is a function of coal mechanical properties, such as modulus, sorption and pore pressure.

2.3.3. Dynamic porosity model for fracture

The porosity of the fracture system with cubic blocks is defined as (Robertson et al., 2006).

$$\phi_f = \frac{3b}{a} \tag{26}$$

where a is the uniform spacing between fractures defining the edge dimension of the REV cubic matrix, and b the fracture aperture as illustrated in Fig. 1. The change in porosity is defined as

$$\Delta\phi_f = \frac{3\ \Delta b}{a} - \frac{3\,\Delta a}{a^2} = \phi_f\left(\frac{\Delta b}{b} - \frac{\Delta a}{a}\right) \tag{27}$$

or

$$\Delta\phi_f = \phi_f(\Delta\varepsilon_f - \Delta\varepsilon_v) \tag{28}$$

where ε_f is the strain within the fracture and ε_v is the volumetric strain of the matrix. Substituting Eq. (22) into Eq. (28), yields,

$$\frac{\Delta\phi_f}{\phi_f} = \frac{\Delta\sigma_e^f}{Kn} - \frac{\Delta\sigma_e^m}{Ks} - \Delta\varepsilon_s. \tag{29}$$

If the initial fracture porosity is ϕ_{f0} at the initial effective stress σ_e^0, the dynamic porosity can be expressed as

$$\phi_f = \phi_{f0}\exp\left[\frac{\sigma_e^f - \sigma_e^{f^0}}{Kn} - \frac{\sigma_e^m - \sigma_e^{m^0}}{Ks} - (\varepsilon_s - \varepsilon_s^0)\right] \tag{30}$$

where $\sigma_e^m = (\sigma_{kk}/3) + \alpha p_m$, $\sigma_e^f = (\sigma_{kk}/3) + \beta p_f$. σ_{kk} is the compressive stress, α, β are the Biot coefficients of matrix and fracture.

2.3.4. Dynamic permeability model for fracture

For the fracture system comprising continuous orthogonal fractures, the cubic law for fracture permeability can be expressed as

$$k_f = \frac{b^3}{12a}. \tag{31}$$

The dynamic permeability of the fracture system can be expressed as

$$\Delta k_f = \frac{3b^2\ \Delta b}{12a} - \frac{b^3\,\Delta a}{12a^2} = k_f\left(\frac{3\,\Delta b}{b} - \frac{\Delta a}{a}\right) \tag{32}$$

or

$$\Delta k_f = k_f\left(3\ \Delta\varepsilon_f - \Delta\varepsilon_v\right) \tag{33}$$

Substituting Eq. (22) into Eq. (33), yields,

$$\frac{\Delta k_f}{k_f} = 3\frac{\Delta\sigma_e^f}{Kn} - \frac{\Delta\sigma_e^m}{Ks} - \Delta\varepsilon_s. \tag{34}$$

If the initial permeability of the fracture system is k_{f0} at the initial effective stress σ_e^0, the permeability can be expressed as

$$k_f = k_{f0}\ \exp\left[3\frac{\sigma_e^f - \sigma_e^{f^0}}{Kn} - \frac{\sigma_e^m - \sigma_e^{m^0}}{Ks} - (\varepsilon_s - \varepsilon_s^0)\right] \tag{35}$$

For this cubic fracture model, the initial porosity and permeability can be calculated by the initial size of matrix block and cleat aperture.

$$\phi_{f0.} = \frac{3b_0}{a_0} \tag{36}$$

$$k_{f0} = \frac{b_0^3}{12a_0} \tag{37}$$

Therefore, Eqs. (19), (25), (30), (35) define the general porosity and permeability model for a dual-porosity medium.

2.4. Coupled field equations

For convenience, the governing equation for coal deformation is re-written as follows:

$$Gu_{i,kk} + \frac{G}{1-2\nu}u_{k,ki} - \alpha p_{m,i} - \beta p_{f,i} - K\varepsilon_L\frac{p_L}{(p_m+p_L)^2}p_{m,i} + f_{,i} = 0 \tag{38}$$

where p_m and p_f are pore pressures in the matrix and fracture, respectively. They can be obtained by solving the field equations for gas flow. Substituting the partial derivatives of ϕ_m and ϕ_f with respect to time from Eqs. (19) and (30) and the permeability equations (25) and (35) into gas flow equations (16) and (17), yields the final gas flow equations:

$$\left[\phi_m + \rho_{ga}\rho_c\frac{V_L p_L}{(p_m+p_L)^2} + \frac{(\alpha-\phi_m)p_m}{(1+S)Ks} - \frac{(\alpha-\phi_m)\varepsilon_L p_L p_m}{(1+S)(p_m+p_L)^2}\right]\frac{\partial p_m}{\partial t} + \nabla\cdot\left(-\frac{k}{\mu}p_m\nabla\cdot p_m\right) = \omega(p_f - p_m) - \frac{(\alpha-\phi_m)p_m}{(1+S)}\frac{\partial\varepsilon_v}{\partial t} \tag{39}$$

$$\phi_f\left(1 + \frac{p_f\beta}{Kn}\right)\frac{\partial p_f}{\partial t} - \phi_f\left(\frac{p_f\alpha}{Ks} + \frac{\varepsilon_L p_L p_m}{(p_m+p_L)^2}\right)\frac{\partial p_m}{\partial t} + \nabla\cdot(-\frac{k}{\mu}p_f\nabla\cdot p_f) = -\omega(p_f - p_m) - p_f\phi_f\left(\frac{1}{Kn} - \frac{1}{Ks}\right)\frac{\partial(\sigma_{kk}/3)}{\partial t} \tag{40}$$

In this study, Eq. (39) is re-arranged as

$$S_g\frac{\partial p_m}{\partial t} - \nabla\cdot\left(\frac{k}{\mu}p_m\nabla p_m\right) = \omega(p_f - p_m) \tag{41}$$

where

$$S_g = S_{g1} + S_{g2} + S_{g3} + S_{g4} + S_{g5} \tag{42}$$

$$S_{g1} = \phi, \quad S_{g2} = \frac{\rho_c p_a V_L p_L}{(p+p_L)^2}, \quad S_{g3} = \phi\frac{(\alpha-\phi)p}{(1+S)Ks},$$

$$S_{g4} = -\frac{(\alpha-\phi)\varepsilon_L p_L p}{(1+S)(p+p_L)^2}, \quad S_{g5} = \frac{(\alpha-\phi)p}{(1+S)}\frac{\partial\varepsilon_v}{\partial p}.$$

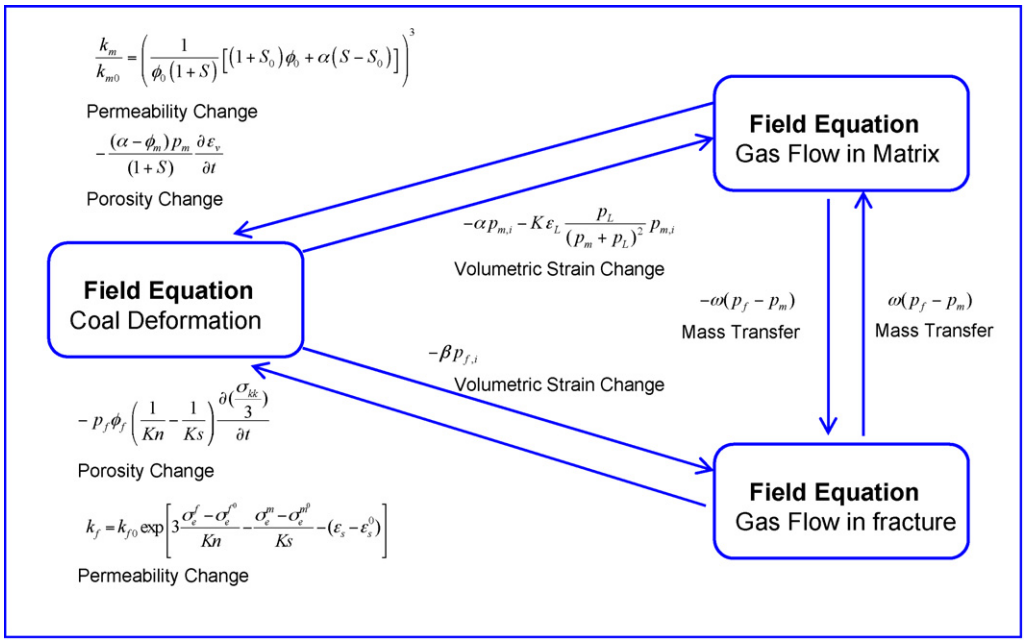

Fig. 3. Cross-couplings between coal deformation equation, gas flow equation in the matrix system and gas flow equation in the fracture system.

where S_g is the gas storativity. S_{g1} through S_{g5} represent each term of the right side of Eq. (42). Gas storativity is defined as the volume of gas released (or sequestered) from storage per unit change in pressure in the gas reservoir, and per unit volume of the reservoir. It consists of five components: S_{g1} is the volume of gas released (or sequestered) from the free-phase gas; S_{g2} is the volume of gas released (or sequestered) from the adsorbed-phase gas; S_{g3} is the volume of gas released (or sequestered) due to the coal grain deformation; S_{g4} is the volume of gas released (or sequestered) due to coal grain shrinking or swelling; S_{g5} is the volume of gas released (or sequestered) due to the bulk (skeletal) deformation of the coal. On the right-hand side, the term is a coupled term with the pressure associated to the gas flow in fracture.

In Eq. (40), the first term of this equation is the gas storage coefficient in the fracture. For the remaining terms, the first is the gas volume resulting from free-phase gas, and the second is the volume resulting from the mechanical deformation of the coal. The sorption-induced strain in the fracture is not considered as the fracture has negligible volume—adsorption only occurs in the matrix. The second term on the left-hand side represents the change in volumetric strain and sorption-induced strain in the matrix, which can also induce a change in gas storage in the fracture. On the right-hand side, the first term is a coupled term with the pressure associated with the gas flow in matrix. The second term is a coupled term including the rate change in the volumetric strain due to coal deformation.

Therefore, Eqs. (38)–(40) define a model for coupled gas flow and coal deformation in dual-porosity medium. Cross-couplings between the field equations of coal deformation and gas flow are illustrated in Fig. 3.

This DP model is more complex than some other single porosity models and those that do not explicitly accommodate displacements. However the required input data are not significantly greater than for "smeared" single porosity "invariant-total-stress models." The input data can be categorized as four types.

(1) *The basic mechanical properties*. These include the Elastic modulus, Poisson's ratio, fracture spacing and initial fracture aperture (from permeability). These parameters can be obtained by laboratory testing.
(2) *The gas flow parameters*. These include permeability of fracture/matrix and the porosity of the fracture/matrix. These parameters can be obtained by laboratory testing.
(3) *The adsorption/desorption properties*. These include Langmuir pressure constant, Langmuir volume constant and Langmuir volumetric strain constant. These parameters can be obtained by laboratory testing.
(4) *The reservoir conditions*. These include the in situ stress conditions and the displacement boundary conditions in the near- and far-field. These are recovered from field observation.

These properties are the basic parameters needed by the model. Some other parameters can be calculated from these parameters. In the normal manner, process-based observations of response result from the application of measured and estimated parameters and their matching with field observations through calibration.

2.5. Boundary and initial conditions

For the Navier-type equation, the displacement and stress conditions on the boundary are given as

$$u_i = \tilde{u}_i(t), \quad \sigma_{ij} n_j = \tilde{F}_i(t) \quad \text{on} \quad \partial\Omega \tag{43}$$

where $\tilde{u}_i(t)$ and $\tilde{F}_i(t)$ are the components of prescribed displacement and stress on the boundary $\partial\Omega$, respectively and n_j is the direction cosine of the vector normal to the boundary. The initial conditions for displacement and stress in the domain Ω are described as

$$u_i(0) = u_0, \quad \sigma_{ij}(0) = \sigma_0 \quad \text{in} \quad \Omega \tag{44}$$

Here, u_0 and σ_0 are initial values of displacement and stress in the domain Ω. For the gas flow equations, the Dirichlet and Neumann boundary conditions are defined as

$$p_m = \tilde{p}_m(t), \quad \vec{n} \cdot \frac{k_m}{\mu} \nabla p_m = \tilde{Q}^f(t) \quad \text{on} \quad \partial\Omega \tag{45}$$

$$p_f = \tilde{p}_f(t), \quad \vec{n} \cdot \frac{k_f}{\mu} \nabla p_f = \tilde{Q}^f_s(t) \quad \text{on} \quad \partial\Omega \tag{46}$$

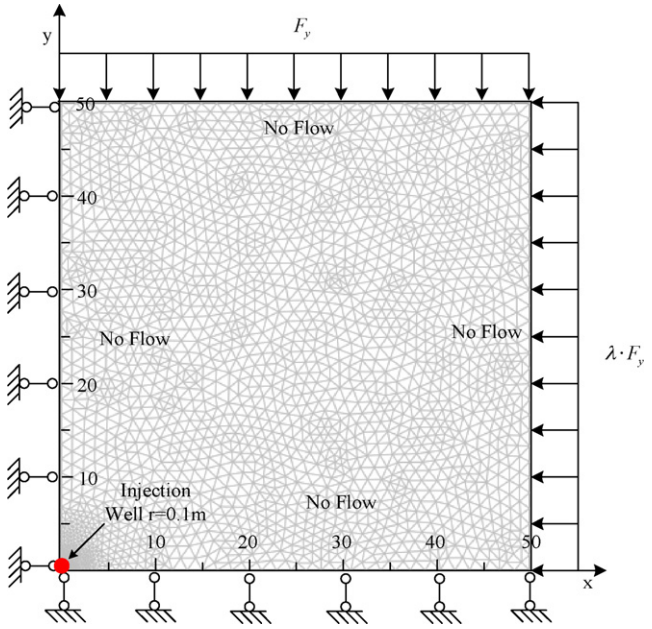

Fig. 4. Quarter simulation model of CO_2 injection to a coal seam.

Here, $\tilde{p}(t)$ and $\tilde{Q}_s(t)$ are the specified gas pressure and gas flux on the boundary. The subscripts m and f represents matrix block and fracture, respectively. The initial conditions for gas flow are

$$p_m(0) = p_{m0}, \quad p_f(0) = p_{f0} \quad \text{in} \quad \Omega. \tag{47}$$

3. Investigation of pressure responses

Eqs. (38)–(40) define the coupled gas flow and coal deformation response through (1) dynamic porosity evolution in the matrix (Eq. (19)) and the (2) fracture system (Eq. (30)); and through (3) dynamic permeability evolution in the matrix (Eq. (25)) and the (4) fracture system (Eq. (35)). The resulting equation system had been solved by use of Comsol Multiphysics, a commercial PDE solver. In the following sections, the results of pressure responses to CO_2 injection are presented.

3.1. Model description and input parameters

In order to investigate the dual poroelastic response of a coal seam to CO_2 injection, a simulation model was constructed as shown in Fig. 4. A quarter of the injection well with a radius of 0.1 m is located at the left-bottom corner of the model. The whole model has 5104 elements in total and the number of degrees of freedom is 41,588 comprising two displacements and two pressures (fracture and matrix) at each node.

Table 1
Property parameters of simulation model.

Parameter	Value
Young's modulus of coal, E (MPa)	2713
Young's modulus of coal grain, E_s (MPa)	8143
Possion's ratio of coal, ν	0.339
Density of coal, ρ_c (kg/m^3)	1400
Density of CO_2, ρ_g (kg/m^3) at standard condition	1.98
Viscosity of CO_2, μ (Pa s)	1.84×10^{-5}
Langmuir pressure constant, P_L (MPa)	6.109
Langmuir volume constant, V_L (m^3/kg)	0.015
Langmuir volumetric strain constant, ε_L	0.02295
Initial porosity of matrix, φ_{m0}	0.02
Initial permeability of matrix, k_{m0} (m^2)	10^{-18}
Fracture aperture, b_0 (m)	1×10^{-4}
Matrix size, a_0 (m)	0.01
Lateral stress ratio, λ	1.5

Appropriate boundary conditions must be applied to this coupled coal deformation and gas flow problem. For the coal deformation model, the left side and base are both rollered and in situ stresses are applied to the top and the right side. The ratio of the horizontal in situ stresses (along page to across page) is kept as 1.5. For gas flow, a constant pressure of 8 MPa is applied to the injection well. No flow conditions are applied to all the other boundaries. An initial pressure of 0.5 MPa is applied in the model. Input properties are listed in Table 1. The values of these properties were chosen from the literature (Robertson and Christiansen, 2005) with the initial porosity and permeability of the fracture system calculated from Eq. (36) and (37).

A series of injection conditions as listed in Table 2 was simulated to investigate the mechanical responses of coal. Simulation results are presented in terms of (1) the impacts of modulus ratio, (2) the impacts of fracture density, and (3) the impacts of in situ stresses on the boundary.

3.2. Simulation results and discussions

3.2.1. Impacts of ratios of the coal bulk modulus to the coal grain modulus

To investigate the impact of skeletal and grain modulii on the resulting response, four simulations were conducted with: (1) $K/K_s = 1/2$ and $\varepsilon_v \neq 0$; (2) $K/K_s = 1/3$ and $\varepsilon_v \neq 0$; (3) $K/K_s = 1/10$ and $\varepsilon_v \neq 0$; (4) $K/K_s = 1/3$ and $\varepsilon_v = 0$. In all these simulations, the fracture spacing is set to $a = 0.01$ m, the in situ stresses to $F_y = -6$ MPa and $F_x = -9$ MPa. Simulation results are shown in Figs. 5–8.

As shown in Eq. (41), there are five contributing mechanisms to the storativity: free gas compression, gas absorption, coal grain deformation, coal shrinking or swelling, and coal bulk (skeletal) deformation. The contribution of each mechanism to the complete gas storativity is shown in Fig. 5. As the matrix pore pressure increases, the volume of gas released (or sequestered)

Table 2
Simulation matrix for the investigation of pressure responses to CO_2 injection under different conditions.

Case 1 Impacts of the ratio of coal bulk modulus to gain modulus on pressure responses to CO_2 injection	$K/K_s = 1/2, \varepsilon_s \neq 0$ $K/K_s = 1/3, \varepsilon_s \neq 0$ $K/K_s = 1/10, \varepsilon_s \neq 0$ $K/K_s = 1/3, \varepsilon_s = 0$
Case 2 Impacts of fracture spacing on pressure responses to CO_2 injection	$a = 0.01, \varepsilon_s \neq 0$ $a = 0.05, \varepsilon_s = 0$ $a = 0.01, \varepsilon_s \neq 0$ $a = 0.05, \varepsilon_s = 0$
Case 3 Impacts of in situ stresses on pressure responses to CO_2 injection	$F_y = -1$ MPa, $F_x = \lambda \cdot F_y$ $F_y = -6$ MPa, $F_x = \lambda \cdot F_y$ $F_y = -12$ MPa, $F_x = \lambda \cdot F_y$

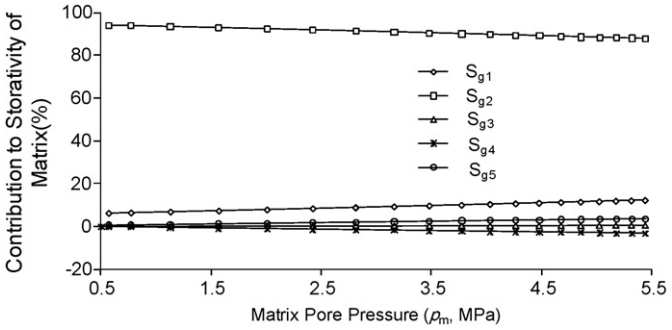

Fig. 5. Contributions of each mechanism to gas storativity in the matrix: S_{g1} is the volume of gas released (or sequestered) from the free-phase gas; S_{g2} is the volume of gas released from the adsorbed-phase gas; S_{g3} is the volume of gas released due to the coal gain deformation; S_{g4} is the volume of gas released due to coal grain swelling; S_{g5} is the volume of gas released (or sequestered) due to coal bulk (skeleton) deformation.

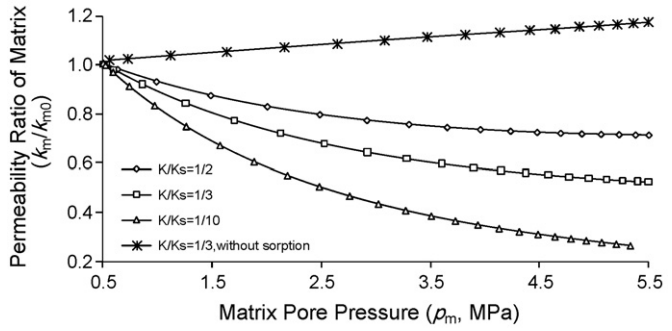

Fig. 6. The relation between matrix permeability ratio and matrix pore pressure at the specific point of $x = 2$ and $y = 2$, adjacent to the wellbore.

from the adsorbed-phase gas contributes about 87.6–93.9% to the total gas storativity. The volume of gas released from the free-phase contributes 6.1–12.2% to the total gas storativity, and that from bulk deformation contributes 0.38–3.44% to the total gas storativity. The contributions from the other mechanisms are less than 3.5% in total. These results indicate that gas sorption is the primary mechanism for gas production or sequestration.

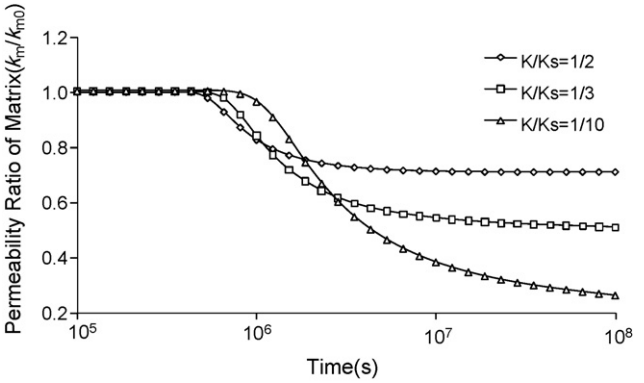

Fig. 7. The evolution of the matrix permeability ratio with time at a specific point of $x = 2$ and $y = 2$ adjacent to the wellbore.

The relation between matrix permeability ratio and matrix pore pressure at a specific point is shown in Fig. 6. For the simulation of $K/K_s = 1/3$ and $\varepsilon_v = 0$ (without sorption), the permeability ratio increases with an increase in the matrix pore pressure as expected with the effective stress dependency. Conversely, for all other simulations, the permeability ratio decreases with an increase in the matrix pore pressure. In these situations, the effective stress effect and the sorption effect are competing: an increase in the matrix pressure (or a decrease in the effective stress) enhances the matrix permeability while an increase in the sorption reduces the matrix permeability. For these particular conditions the resultant effect is a monotonic decrease in permeability with increasing pressure as the effects of sorption-induced swelling dominate.

The evolution of the matrix permeability ratio with time at a specific point is shown in Fig. 7. At early time, when there is little influence of sorption, the matrix permeability remains almost unchanged. As sorption increases, the matrix permeability decreases until the gas uptake reaches a final equilibrium. For all three cases of mechanical response, the evolution of per-

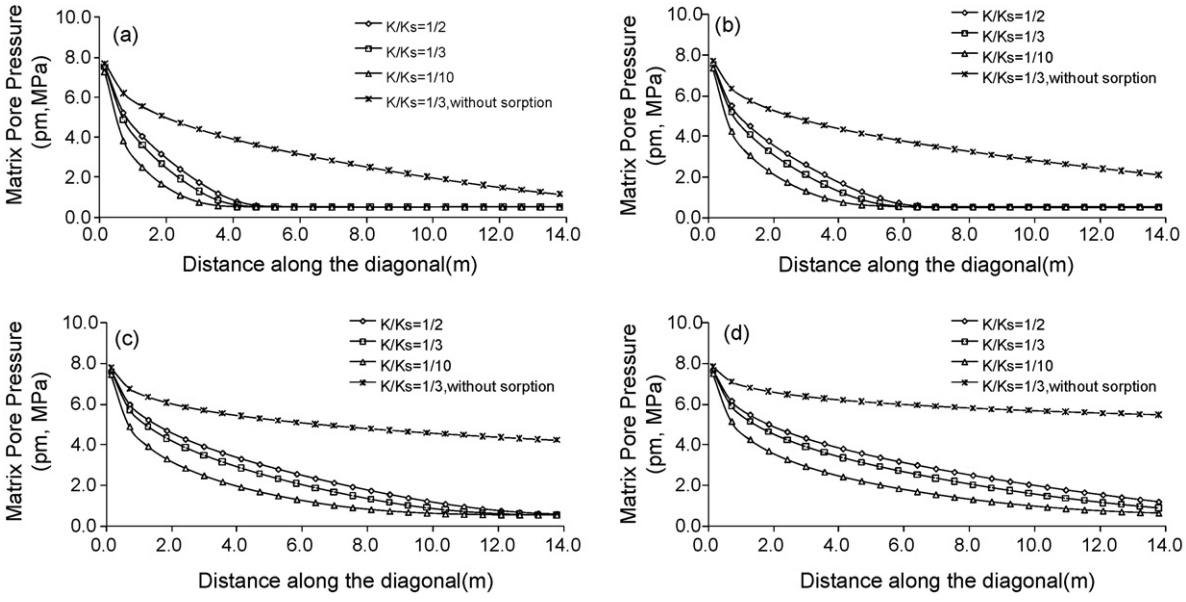

Fig. 8. The distribution of matrix pressure (p_m) along a radius outward from the wellbore (the diagonal line $y = x$) for different modulus ratios: (a) $t = 5 \times 10^6$ s; (b) $t = 1 \times 10^7$ s; (c) $t = 5 \times 10^7$ s; (d) $t = 1 \times 10^8$ s.

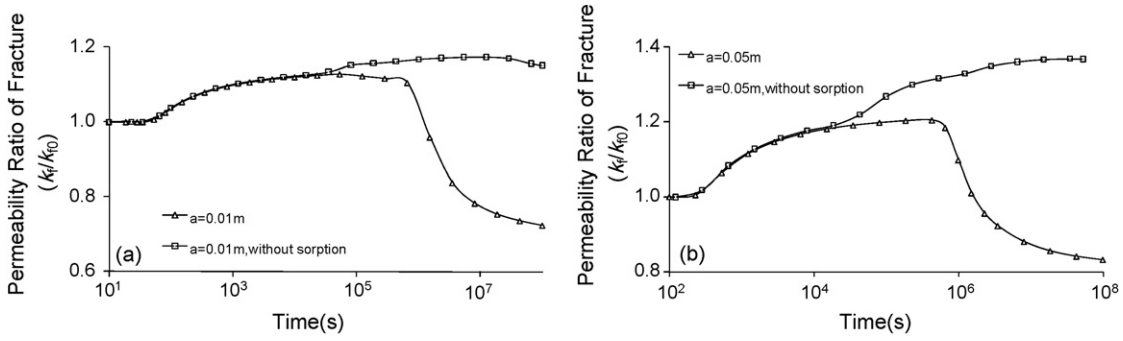

Fig. 9. The evolution of fracture permeability ratio with time at a specific location close to the wellbore ($x = 2$ and $y = 2$) for the cases of $a = 0.01$ m and $a = 0.05$ m.

meability follows a similar trend but is regulated by the various modulus ratios. For example, the permeability ratio decreases with increasing pore pressure. The ultimate permeability ratios at steady state are in the range 0.71 ($K/K_s = 0.5$) to 0.26 ($K/K_s = 0.1$) when $t = 10^8$ s. This can be explained through Eq. (8). The greater the modulus ratio, the smaller the Biot coefficient α. Since the Biot coefficient measures the effect of pore pressure on the coal deformation, the greater value of bulk modulus ratio results in smaller ultimate permeability ratio of matrix.

The spatial and temporal variations of the pore pressure in matrix are shown in Fig. 8(a)–(d). These results show that the permeability modification profiles propagate outward from the source of the pressure perturbation (the borehole) with time. The rates of propagation and the ultimate permeability ratios are again modulated by the modulus ratios. The greater the modulus ratio, the faster the CO_2 diffuses into the matrix block, indicating that the Biot coefficient has a significant effect on CO_2 transport.

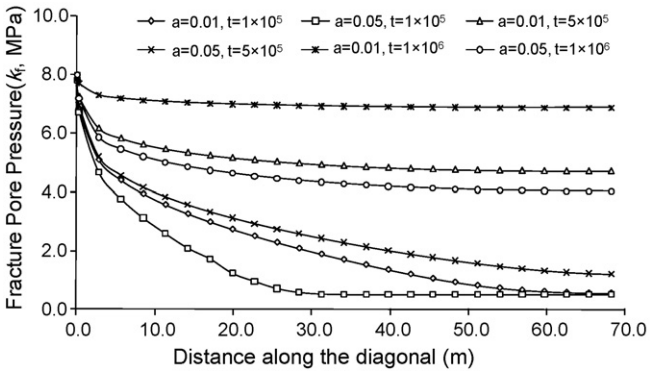

Fig. 11. The distribution of fracture pressure (p_f) along a radius outwards from the wellbore (the diagonal $y = x$) for different times.

3.2.2. Impacts of fracture spacing

Four simulations were conducted: (1) $a = 0.01$ m and $\varepsilon_v \neq 0$; (2) $a = 0.05$ m and $\varepsilon_v \neq 0$; (3) $a = 0.01$ m and $\varepsilon_v \neq 0$; (4) $a = 0.05$ m and $\varepsilon_v = 0$. In all these simulations, the modulus ratio is assumed equal to $K/K_s = 1/3$ and the in situ stresses as $F_y = -6$ MPa and $F_x = -9$ MPa. Simulation results are shown in Figs. 9–14.

These analyses demonstrate the competitive changes in permeability in the fractures and matrix as the coal matrix swells. As fracture pressures are initially increased, effective stresses are reduced and fracture permeabilities concomitantly increased (Fig. 10). Although gas pressures remain elevated, the evolution of sorption in the matrix results in swelling, which ultimately reduces fracture permeability as total stresses in the near wellbore ultimately build, even as fluid pressures remain constant (Fig. 10). This process begins around 10^6 s, congruent with the results for the matrix, noted in Fig. 7. The key influence of sorption-induced swelling in augmenting total stresses is inferred from Fig. 10 where absent swelling, fracture permeabilities are always increased with an increase in pore pressure. This influence of swelling-induced changes in total stresses is a key component of this analysis that cannot be accommodated where mechanical effects are only incorporated approximately for assumed constant total stresses.

For the case of CO_2 injection, an increase in the matrix pressure (or an increase in the gas sorption) reduces the fracture permeability significantly. Ultimate response is also conditioned by the Biot coefficient, α—as the Biot coefficient decreases (increasing matrix

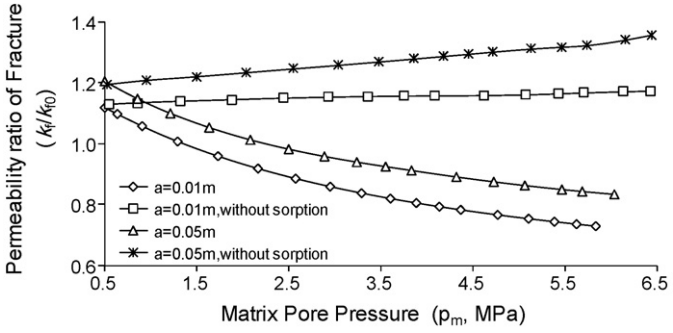

Fig. 10. The evolution of fracture permeability ratio with matrix pore pressure close to the wellbore ($x = 2$ and $y = 2$) for all four cases.

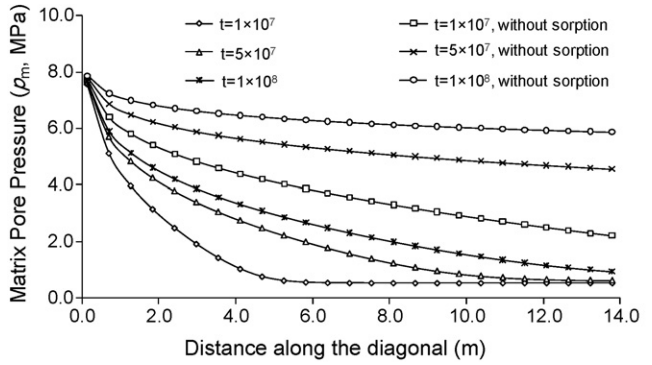

Fig. 12. The distribution of matrix permeability ratio a radius outward from the wellbore (along the diagonal $y = x$) for different times.

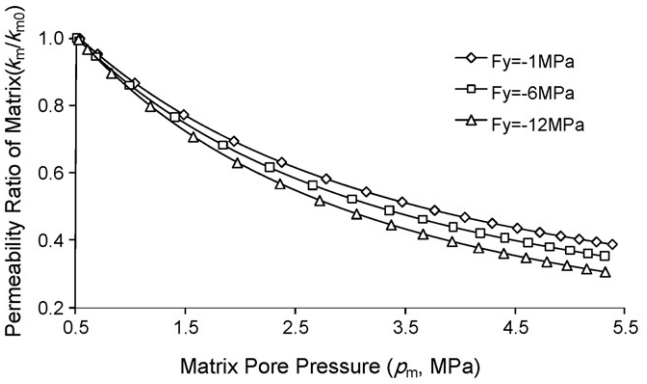

Fig. 13. The relation between matrix permeability ratio and matrix pore pressure close to the wellbore ($x = 2$ and $y = 2$) for different in situ stresses.

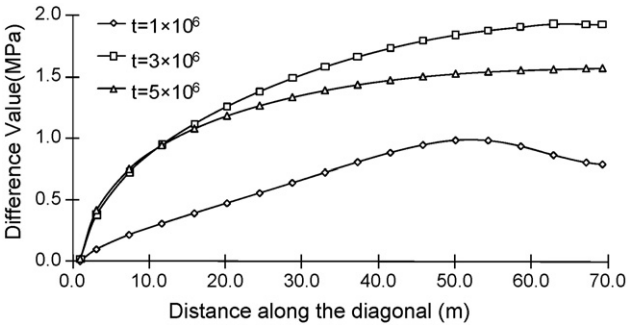

Fig. 15. The distribution of the differential value between pore pressure for the case of $F_y = -1$ MPa and that for the case of $F_y = -12$ MPa under three different times.

modulus ratio) the influence of pore pressure on coal deformation, and hence on permeability change is reduced.

The evolutions of spatial changes of pore pressure in the fracture are shown in Fig. 11, indicating more rapid transport where the fracture density is large. Similarly, where the fracture system effectively transports CO_2 into the core of the domain, far from the wellbore, the pore pressures within the matrix are able to respond more quickly, with the relatively short diffusion length (Fig. 12).

3.2.3. *Impacts of in situ stresses*

Three simulations were conducted: (1) $F_y = -1$ MPa and $F_x = -1.5$ MPa; (2) $F_y = -6$ MPa and $F_x = -9$ MPa; (3) $F_y = -12$ MPa and $F_x = -18$ MPa. In all these simulations, the modulus ratio is assumed as $K/K_s = 1/3$. Simulation results are shown in Figs. 13–15.

The evolution of ultimate permeability is weakly linked to initial stress magnitude, as illustrated in Fig. 13. Higher initial stresses provide greater confinement and result in a slight decrease in ultimate permeability. The boundary conditions selected here are for a single injector in an infinite two-dimensional medium. If injection is completed on a grid, then the stress boundary conditions would be replaced by rollered sides, and ultimate reductions in permeability would be greater. The ultimate permeability reductions for a single well are of the order of 0.31 at 12 MPa and 0.45 at 1 MPa, suggesting that injection is progressively more difficult as initial in situ stresses increase.

The pore pressure distributions within fracture at different points in time are shown in Fig. 14. It can be seen from these figures that the CO_2 transport under small overburden loads is much more rapid than at elevated initial stresses. This results as low stresses allow higher fracture permeabilities which in turn allow more rapid transport of CO_2 to the extremities of the reservoir. Once supplied to the distal portions of the reservoir, sorption is controlled by the diffusive length-scale of the matrix block edge dimension (fracture spacing). The differences in pore pressure for two uniform stress states of 1 and 12 MPa at different points in time are shown in Fig. 15. The greatest difference in pore pressure was obtained at 3×10^6 s. This means that at the beginning the gas pressure increases much faster under small in situ stress under large in situ stress.

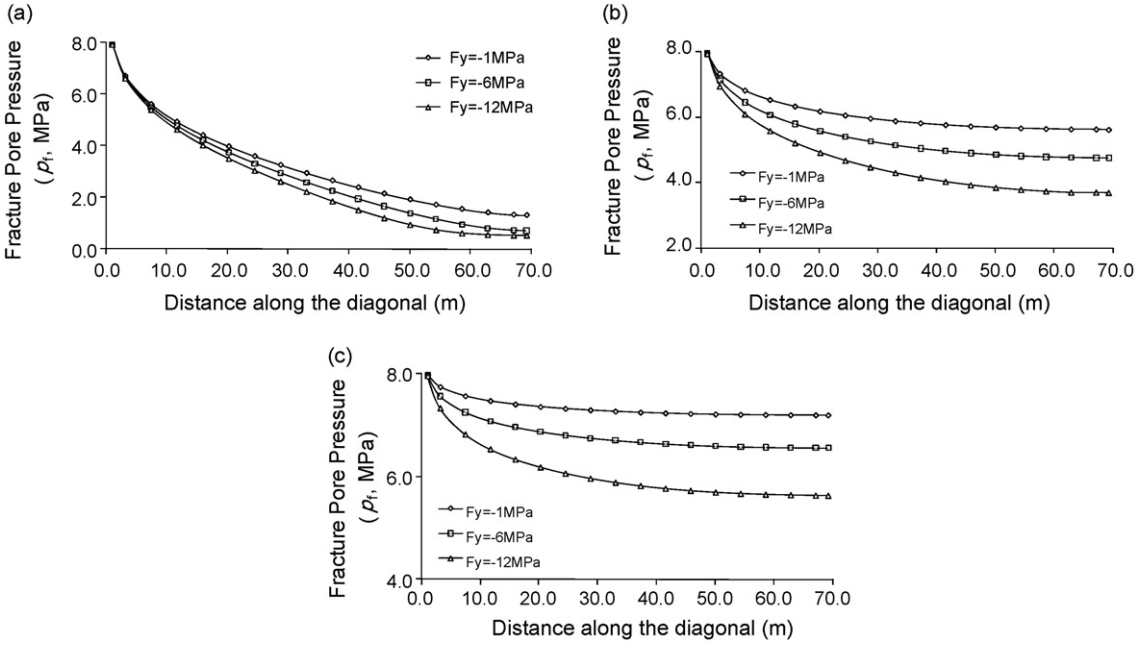

Fig. 14. The distribution of fracture pore pressure radially outward from the wellbore (along the diagonal $y = x$) for different in situ stresses: (a) $t = 1 \times 10^6$ s; (b) $t = 3 \times 10^6$ s; (c) $t = 5 \times 10^6$ s.

4. Conclusions

In this study, a novel dual poroelastic model is developed to quantify the dynamics of CO_2 injection into coal. The model separately accommodates compressible gas flow and transport in the coal matrix and fracture systems and rigorously accommodates the role of mechanical deformations for a dual-porosity continuum. Since mechanical interactions and the role of sorption-induced strains are rigorously accommodated, micro-mechanical models are capable of recovering the evolution of porosity and permeability in both the coal matrix and the fracture network. This linearized model represents important non-linear responses due to the completion between effective stress and sorptive effects that cannot be recovered where mechanical influences are not rigorously coupled with the transport system. Major findings are summarized as follows:

(1) Unlike the flow of slightly compressible fluids where no sorption is included, the gas sorption for this study is the primary mechanism for either gas production or sequestration. In this dual poroelastic model, there are five contributing mechanisms to the storativity, namely: free gas compression, gas absorption, coal grain deformation, coal shrinkage/swelling, and bulk skeletal deformation of the coal. Our simulation results indicate that the volume of gas released (or sequestered) from the adsorbed-phase contributes about 90% to the total gas content.
(2) Unlike dual poroelastic models for the flow of slightly compressible fluids where the coal grain modulus can be assumed large in comparison to the skeletal modulus, the coal grain modulus for this study may have significant impacts on response. Model results indicated that the permeability of the matrix is mainly affected by sorption-induced coal deformation. The grain modulus is an important parameter that affects the evolution of permeability when adsorption is taken into consideration. The greater the ratio of coal bulk modulus to coal grain modulus, the more rapid the reduction in matrix permeability ratio.
(3) Unlike the flow of slightly compressible fluids in inert media where the fracture permeability typically increases with an increase in pore pressure in the fracture, this study illustrates a counter influence of sorption. Early-time increases in permeability in response to elevated fracture pressures are lost and ultimately reversed as sorption-induced changes in permeability swell the matrix, locally increase total stresses, and elevate effective stresses. The timing of this reversal in response is conditioned by the diffusive timescale conditioned by the ratio of fracture spacing squared to the sorptive diffusivity of the coal matrix.

Changes in permeability are shown to be important and fast acting. Permeability may be reduced by an order of magnitude from the initial permeability and these changes act within the design lives of typical projects (days to years). End member behaviors for stress or displacement boundary conditions may be recovered directly from the constitutive relations. Where local total stress conditions are applied, permeability at steady state will increase for both matrix and fracture system in response to injection. Where strains are constrained, injection-induced permeabilities within the fracture will initially increase and subsequently decrease as sorptive stresses build. Where restraints are mixed, the response will be defined both by the constitutive behavior and local stress equilibrium, requiring that full solution of the coupled equations is completed. Thus, for accurate and reliable predictions of the response to gas injection in sorptive media, a fully coupled model linking transport, sorption and deformation must be employed.

Acknowledgements

This work was supported by WA:ERA and by NISOH under contract 200-2008-25702. It was also supported by National Basic Research Program of China (2007CB209400) and by the State Key Laboratory for Geomechanics and Deep Underground Engineering, China University of Mining and Technology. These supports are gratefully acknowledged.

References

Aifantis, E.C., 1977. Introducing a multi-porous medium. Dev. Mech. 37, 265–296.
Bai, M., Elsworth, D., 1994. Modeling of subsidence and stress-dependent hydraulic conductivity of intact and fractured porous media. Rock Mech. Rock Eng. 27, 209–234.
Bai, M., Elsworth, D., 2000. Coupled Processes in Subsurface Deformation, Flow and Transport. ASCE Press, 336 pp.
Bai, M., Elsworth, D., Roegiers, J.-C., 1993. Multi-porosity/multi-permeability approach to the simulation of naturally fractured reservoirs. Water Resour. Res. 29, 1621–1633.
Bai, M., Roegiers, J.-C., Elsworth, D., 1995. Poromechanical response of fractured-porous rock masses. J. Petrol. Sci. Eng. 13, 155–168.
Bai, M., Elsworth, D., Inyang, H.I., Roegiers, J.-C., 1997. A semi-analytical solution for contaminant migration with linear sorption in strongly heterogeneous media. J. Environ. Eng. ASCE 123, 1116–1125.
Barenblatt, G.I., Zheltov, I.P., Kochina, N., 1960. Basic concepts in the theory of seepage of homogeneous liquids in fissured rocks. Prikl. Mat. Mekh. 24 (5), 852–864.
Biot, M.A., 1941. General theory of three-dimensional consolidation. J. Appl. Phys. 12, 155–164.
Clarkson, C.R., Bustin, R.M., 1999a. The effect of pore structure and gas pressure upon the transport properties of coal: a laboratory and modeling study. 1. Isotherms and pore volume distributions. Fuel 78, 1333–1344.
Clarkson, C.R., Bustin, R.M., 1999b. The effect of pore structure and gas pressure upon the transport properties of coal. 2. Adsorption rate modeling. Fuel 78, 1345–1362.
Cui, X., Bustin, R.M., 2005. Volumetric strain associated with methane desorption and its impact on coalbed gas production from deep coal seams. AAPG Bull. 89, 1181–1202.
Cui, X., Bustin, R.M., Dipple, Gregory, 2004. Selective transport of CO_2, CH_4, and N_2 in coals: insights from modeling of experimental gas adsorption data. Fuel 83, 293–303.
Douglas Jr., Jim, Hensley, Jeffrey L., Arbogast, Todd, 1991. A dual-porosity model for water flooding in naturally fractured reservoirs. Comput. Methods Appl. Mech. Eng. 87, 157–174.
Elsworth, D., Bai, M., 1992. Flow-deformation response of dual-porosity media. J. Geotech. Eng. ASCE 118, 107–124.
Faiz, M., Saghafi, A., Sherwood, N., Wang, I., 2007. The influence of petrological properties and burial history on coal seam methane reservoir characterisation, Sydney Basin, Australia. Int. J. Coal Geol. 70, 193–208.
Gale, John, Freund, Paul, 2001. Coal-bed methane enhancement with CO_2 sequestration worldwide potential. Environ. Geosci. 8 (3), 210–217.
Gray, I., 1987. Reservoir engineering in coal seams. Part 1. The physical process of gas storage and movement in coal seams. Paper SPE 12514. SPE Reservoir Eng. (February), 28–34.
Harpalani, S., Chen, G., 1997. Influence of gas production induced volumetric strain on permeability of coal. Geotech. Geol. Eng. 15, 303–325.
Harpalani, S., Schraufnagel, A., 1990. Measurement of parameters impacting methane recovery from coal seams. Int. J. Miner. Geol. Eng. 8, 369–384.
Liu, J., Elsworth, D., 1998. Three-dimensional effects of hydraulic conductivity enhancement and desaturation around mined panels. Int. J. R. Mech. Min. Sci. Geomech. Abstr. 34 (8), 1139–1152.
Liu, J., Elsworth, D., 1999. Evaluation of pore water pressure fluctuation around an advancing long wall panel. Adv. Water Res. 22 (6), 633–644.
Liu, J., Elsworth, D., Brady, B.H., 1999. Linking stress-dependent effective porosity and hydraulic conductivity fields to RMR. Int. J. Rock Mech. Miner. Sci. 36, 581–596.
Ouyang, Z., Elsworth, D., 1993. Evaluation of groundwater flow into mined panels. Int. J. Rock Mech. Miner. Sci. Geomech. Abstr. 30, 71–80.
Palmer, I., Mansoori, J., 1998. How permeability depends on stress and pore pressure in coalbeds: a new model. Paper SPE 52607. SPE Reservoir Eval. Eng. (December), 539–544.
Pekot, L.J., Reeves, S.R., 2003. Modeling the effects of matrix shrinkage and differential swelling on coalbed methane recovery and carbon sequestration. Paper 0328. In: Proceedings of the 2003 International Coalbed Methane Symposium, University of Alabama, Tuscaloosa, Alabama, May 2003.
Pili, Eric, Perrier, Frederic, Richon, Patrick, 2004. Dual porosity mechanism for transient groundwater and gas anomalies induced by external forcing. Earth Planet. Sci. Lett. 227, 473–480.
Robertson, E.P., Christiansen, R.L., 2005. Modeling permeability in coal using sorption-induced strain data. Paper SPE 97068. In: Proceedings of the 2005 SPE Annual Technical Conference and Exhibition, Dallas, 9–12 October.

Robertson, Eric P., Christiansen, Richard L., 2006. A permeability model for coal and other fractured, sorptive-elastic media. Paper SPE 104380. In: Proceedings of the 2006 SPE Eastern Regional Meeting, Ohio, 11–13 October.

Sawyer, W.K., 1990. Development and application of a 3D coalbed simulator. Paper CIM/SPE 90-119. In: Presented at the 1990 International Technical Meeting Hosted Jointly by the Petroleum Society of CIM and the Society of Petroleum Engineers, Calgary, Alberta, Canada, 10–13 June.

Seidle, J.P., Huitt, L.G., 1995. Experimental measurement of coal matrix shrinkage due to gas desorption and implications for cleat permeability increases. Paper SPE 30010. In: Presented at the 1995 International Meeting on Petroleum Engineering, Beijing, China, 14–17 November.

Shi, J.Q., Durucan, S., 2003. Changes in Permeability of Coalbeds During Primary Recovery. Part 1. Model Formulation and Analysis. Paper 0341. In: Proceedings of the 2003 International Coalbed Methane Symposium, University of Alabama, Tuscaloosa, Alabama, May.

Shi, J., Durucan, S., 2005. A model for changes in coalbed permeability during primary and enhanced methane recovery. SPE Reservoir Eval. Eng. 8, 291–299.

Warren, J.E., Root, P.J., 1963. Behavior of naturally fractured reservoirs. Trans. AIME, Soc. Petrol. Eng. J. 228 (September), 245–255.

Zhang, H.B., Liu, J., Elsworth, D., 2008. How sorption-induced matrix deformation affects gas flow in coal seams: a new FE model. Int. J. Rock Mech. Mining Sci. 45, 1226–1236.

Zhao, Y.S., Hu, Y.Q., Zhao, B., Yang, D., 2004. Nonlinear coupled mathematical model for solid deformation and gas seepage in fractured media. Transport Porous Media 55, 119–136.